Science of the Total Environment 634 (2018) 224–234

Contents lists available at ScienceDirect

Science of the Total Environment

journal homepage: www.elsevier.com/locate/scitotenv

Efficiency of surfactant-enhanced bioremediation of aged polycyclic aromatic hydrocarbon-contaminated soil: Link with bioavailability and the dynamics of the bacterial community

Martina Cecotti [a], Bibiana M. Coppotelli [a], Verónica C. Mora [a], Marisa Viera [b], Irma S. Morelli [a,c,*]

[a] Centro de Investigación y Desarrollo en Fermentaciones Industriales, CINDEFI (UNLP; CCT-La Plata, CONICET), La Plata, Argentina
[b] Centro de Investigación y Desarrollo en Tecnología de Pinturas, CIDEPINT (CICPBA, CCT-La Plata, CONICET), La Plata, Argentina
[c] Comisión de Investigaciones Científicas de la Provincia de Buenos Aires, La Plata, Argentina

HIGHLIGHTS

- PAH degradation was enhanced by surfactant at sub-CMC doses in aged-contaminated soil.
- Soil bacterial community dynamics were changed by all tested surfactant doses.
- PAH degradation was negatively affected by a selected bacterial community at CMC dose.
- SEBR economic cost would be reduced by the application of sub-CMC doses.

GRAPHICAL ABSTRACT

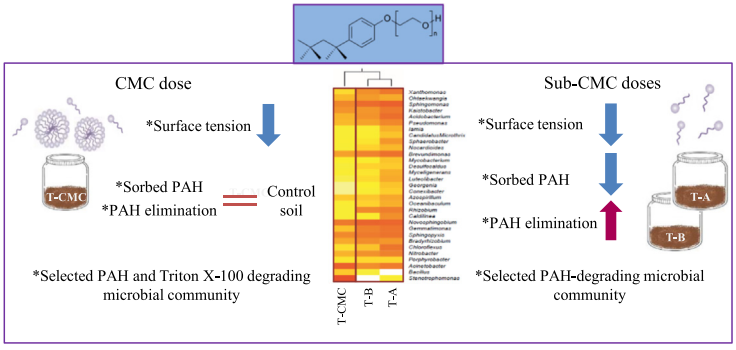

ARTICLE INFO

Article history:
Received 29 January 2018
Received in revised form 18 March 2018
Accepted 24 March 2018
Available online xxxx

Editor: Jay Gan

Keywords:
PAHs
Triton X-100
Biodegradation
Desorption
Pyrosequencing

ABSTRACT

Shifts in the bacterial-community dynamics, bioavailability, and biodegradation of polycyclic aromatic hydrocarbons (PAHs) of chronically contaminated soil were analyzed in Triton X-100–treated microcosms at the critical micelle concentration (T-CMC) and at two sub-CMC doses. Only the sub-CMC-dose microcosms reached sorbed-PAH concentrations significantly lower than the control: 166 ± 32 and 135 ± 4 mg kg^{-1} dry soil versus 266 ± 51 mg kg^{-1}; consequently an increase in high- and low-molecular-weight PAHs biodegradation was observed. After 63 days of incubation pyrosequencing data evidenced differences in diversity and composition between the surfactant-modified microcosms and the control, with those with sub-CMC doses containing a predominance of the orders Sphingomonadales, Acidobacteriales, and Gemmatimonadales (groups of known PAHs-degrading capability). The T-CMC microcosm exhibited a lower richness and diversity index with a marked predominance of the order Xanthomonadales, mainly represented by the *Stenotrophomonas* genus, a PAHs- and Triton X-100–degrading bacterium. In the T-CMC microcosm, whereas the initial surface tension was 35 mN m^{-1}, after 63 days of incubation an increase up to 40 mN m^{-1} was registered. The previous observation and the gas-chromatography data indicated that the surfactant may have been degraded at the CMC by a highly selective bacterial community with a consequent negative impact on PAHs biodegradation. This work obtained strong evidence for the involvement of physicochemical and biologic influences determining the different behaviors of the studied microcosms. The results reported here contribute significantly to an optimization of, surfactant-enhanced bioremediation strategies for chronically contaminated soil since the application of doses below the CMC would reduce the overall costs.

* Corresponding author at: CINDEFI, Calle 50 N°227, 1900 La Plata, Argentina.
E-mail address: guri@biol.unlp.edu.ar. (I.S. Morelli).

https://doi.org/10.1016/j.scitotenv.2018.03.303

1. Introduction

Bioremediation is an economically and environmentally friendly alternative for the clean-up of soil contaminated by recalcitrant pollutants such as polycyclic aromatic hydrocarbons (PAHs) (Lladó et al., 2015). Although most PAHs (especially those of low molecular weight) are biodegradable in the presence of a suitable microbial community, these compounds represent the main chemicals whose particular limitation in bioremediation exists because of low bioavailability (Ortega-Calvo et al., 2013). Bioavailability processes have been defined as the individual physical, chemical, and biologic interactions that determine the exposure of chemicals to the organisms associated with soils and sediments (Ren et al., 2017). Because, a low PAHs bioavailability in a contaminated environment must limit the availability of the substrate to microorganisms during bioremediation, a suitable strategy for enhancing bioavailability becomes necessary.

Surfactant-enhanced bioremediation (SEBR) is a promising chemical technology for improving the accessibility of the pollutants (Ortega-Calvo et al., 2013). When the concentration of a surfactant (amphiphilic molecule) is above the critical micelle concentration (CMC), micellar aggregates provide an additional available hydrophobic area within the central region of the constituent micelles that enhances the solubility of PAHs in an aqueous bulk solution (Mao et al., 2015). In addition to micellar solubilization, certain authors have proposed another possible mechanism involving a modification of the contaminant matrix (Adrion et al., 2016; Bezza and Chirwa, 2017; Singleton et al., 2016). This latter mechanism usually would occur at doses below the CMC through an increase in PAHs diffusivity (Adrion et al., 2016) and a decrease in interfacial tension; thus changing the wettability of the system (Bezza and Chirwa, 2017; de la Cueva et al., 2016), and in so doing, enhancing the separation of the pollutant from the soil particles.

In general, the nonionic surfactants exhibit higher hydrocarbon solubilization than cationic and anionic ones (Lamichhane et al., 2017). Thus, nonionic surfactants are the most frequently used in biodegradation approaches, mainly because of the absence of an electrical charge in the surfactant molecule—minimizing possible toxic effects—along with the generally lower CMC compared to those of cationic or anionic surfactants (Bueno-Montes et al., 2011). The application of nonionic surfactants during soil bioremediation has thus been studied extensively (de la Cueva et al., 2016; Lamichhane et al., 2017). Different SEBR strategies, however, have exhibited inconsistent effects, depending on the properties of the soil and pollutant and on the surfactant type and concentration. Certain studies have reported positive results with SEBR (Adrion et al., 2016; Bueno-Montes et al., 2011; Singleton et al., 2016; Sun et al., 2012; Wang et al., 2016; Yu et al., 2011; Zhu and Aitken, 2010), but others have registered negligible and/or negative effects (Colores et al., 2000; Ghosh and Mukherji, 2016; Liu et al., 2016; Lladó et al., 2013). The possible reasons for the negative findings include the utilization of the surfactant as a carbon and energy source in preference to the contaminants (Colores et al., 2000), a toxicity to the PAHs-degrading bacteria at surfactant supra-CMCs (Lladó et al., 2013; Mao et al., 2015), and a low availability of PAHs to microorganisms once in the micellar phase (de la Cueva et al., 2016; Makkar and Rockne, 2003).

In addition to the possible mechanisms previously described for surfactant action in solubilizing of contaminants, PAHs biodegradation could be affected by the action of surfactants on the dynamics of the microbial community (Adrion et al., 2016; Colores et al., 2000; Zhu and Aitken, 2010). Recently the use of the molecular-biology–fingerprinting technique (PCR-DGGE) along with high-throughput DNA-sequencing have pointed to the conclusion that surfactant addition to PAHs-contaminated soils causes dramatic shifts in the microbial populations present (Colores et al., 2000; Wang et al., 2016), even under sub-CMC conditions (Colores et al., 2000), thus demonstrating the necessity to study the effect of surfactants on the complex microbial communities in PAHs-polluted soils in order to optimize the SEBR.

The aim of this study was therefore to ascertain the link between the population dynamics of the soil bacterial community, as determined by high-throughput sequencing of 16S rRNA amplicons of soil DNA and quantitative real-time PCR, and the efficiency of the SEBR strategy at different concentrations of Triton X-100 in PAHs-aged contaminated soil microcosms. Concentrations of Triton X-100 both at and below the CMC (determined on soil suspensions) were tested.

2. Materials and methods

2.1. Chemicals

The nonionic surfactant used was the octylphenol ethoxylate ether Triton X-100 (ultrapure, USB Corporation, USA), with an average number of ethylene-oxide units around 9.5, corresponding to an average molecular weight of 625 g mol^{-1}. The polymeric adsorbent resin Amberlite XAD-2 (20–60 mesh) was supplied by Sigma Aldrich, USA. The hydrocarbon extraction was performed with acetone and dichloromethane (Sintorgan, Argentina). Dibenzothiophene (Sigma Aldrich, USA) was used as an internal standard for the quantitative analysis of hydrocarbons. The PAHs were identified through comparison with the commercial standard solutions supplied by Restek, USA.

2.2. Aged PAH-contaminated soil

The soil (IPK) used for these assays—removed from a site located within a petrochemical plant in the suburb of the city of Ensenada, Argentina—had been used for a Land-Farming treatment of an area containing petrochemical sludge involving several applications of the treatment over a period of 2 years. The present samples were taken >10 years after that process was over. At the laboratory the sample was sieved (2-mm mesh) and the microcosms assembled within 48 h thereafter.

The physicochemical properties of the soil, upon analysis in the Laboratory of Soil Science at the University of La Plata, were loam at pH 7.71; organic carbon, 2.20%; organic matter, 3.78%; total nitrogen, 0.20%; available phosphorus, 0.00083%; and PAHs, as detected by gas chromatography (GC), 574 ± 138 mg kg^{-1}. The concentration of PAHs of low molecular weight (LMW) and high molecular weight (HMW) was 302 ± 84 mg kg^{-1} and 272 ± 54 mg kg^{-1}, respectively.

2.3. CMC of Triton X-100 in IPK soil

The CMC of Triton X-100 in the soil was assessed by measuring the surface tension of soil suspensions with different surfactant concentrations, as described in (Bueno-Montes et al., 2011). The CMC was determined from supernatants obtained after centrifuging (4000 rpm, 10 min) soil suspensions (2.8 g 70 ml) in distilled water that had been equilibrated with different surfactant concentrations in a 24 h incubation at room temperature with agitation in a rotary shaker. The surface tension was determined at room temperature with a Du Nouy tensiometer (F.B.R., Argentina) for each supernatant in triplicates. The means for each concentration analyzed were plotted in mN m^{-1} as a function of the logarithm of the surfactant concentration in mg l^{-1}. The CMC was calculated as the lowest surfactant concentration not leading to a significant decrease in surface tension.

2.4. Microcosm design and treatment conditions

The soil microcosms—consisting of 500 g of sieved soil (20% moisture content) in a glass container of 1 kg capacity—were assembled in triplicate under four different conditions: (1) C, without surfactant as a control for natural attenuation; (2) T-CMC, with Triton X-100 at 26 mg g^{-1} of dry soil; (3) T-B, with Triton X-100 at 14 mg g^{-1} of dry soil; (4) T-A, with Triton X-100 at 11 mg g^{-1} of dry soil. The surfactant was added in aqueous solution, while the same volume of distilled water was added to the C microcosm to standardize the moisture content. All the microcosms were incubated at 24 ± 2 °C for 84 days and were stirred weekly for aeration. When necessary, the moisture content of the soil was corrected to 20 ± 2% by adding distilled water.

Soil samples were collected 1 day after the addition of the surfactant; every 7 days during the first 28 days of the treatment; and later after 42, 63, and 84 days. Twenty grams of soil (wet weight) were collected from each microcosm for the experiments at each sampling time. At the end of the treatment, 160 g were extracted from each microcosm.

2.5. Microbial enumeration

To determine the total cultivable heterotrophic bacteria, 10 g (wet weight) of soil were suspended in 100 ml of 0.85% (w/v) NaCl, homogenized for 30 min on a rotary shaker (250 rpm), and then decanted after 5–10 min. Samples (0.1 ml) of 10-fold dilutions were spread on plates containing R2A medium to count heterotrophic bacteria (Reasoner and Geldreich, 1985). The agar plates were incubated at 24 ± 2 °C for 7 days.

2.6. Surface tension of soil suspensions

The changes in the surface tension of soil suspensions from the microcosms were monitored during the entire treatment. As described in Section 2.3 above, the supernatants of the soil suspensions were removed and the surface tension measured with a Du Nouy tensiometer.

2.7. Quantification of total and sorbed PAHs

For the determination of total PAHs, the ultrasonic extraction EPA SW-846 3550C Method was used. Of the weighed soil, 2.5 g were mixed with 5 g of anhydrous sodium sulfate to form a free-flowing powder. Three sequential extractions were performed with 8 ml of acetone/dichloromethane 1/1 (v/v) as described in (Mora et al., 2014). In each step, the hydrocarbons were extracted in an ultrasonic bath (Testlab Ultrasonic TB10TA) at 40 kHz, 400 W for 60 min (Luque-García and Luque De Castro, 2003). The mixture was centrifuged at 4000 rpm for 10 min (Presvac model DCS-16 RV) and the supernatants collected in a jar for evaporation. The extract was resuspended in 1 ml of dichloromethane and filtered (nylon membrane of 0.45-μm pore size). Before injecting the sample into a Perkin Elmer Clarus 500 gas chromatograph equipped with a flame ionization detector, an internal standard was added (dibenzothiophene) to correct for minor variations in the injection volume. Then 5 μl were injected and analyzed according to (Morelli et al., 2005). The retention times of the different hydrocarbons were determined with standard solutions and quantifications performed with corrections based on the dibenzothiophene results.

The sorbed PAHs was determined by the technique involving adsorption onto previously washed and activated (Medina et al., 2017) Amberlite–XAD-2 resin (Northcott and Jones, 2001). Of this resin, 2 g were placed onto a closed cylindrical steel mesh (260-μm). In addition, 3 g of soil were transferred to a 120-ml glass centrifuge tube. Thirty milliliter of a solution containing 10 mM $CaCl_2$, 10 mM NaN_3 were then added to the centrifuge tube and the cylinder immersed in the solution. The tubes were sealed and incubated with shaking (150 rpm) at room temperature. When the cylinder was removed after 7 days, the PAHs remaining in the soil aqueous phase corresponded to the sorbed fraction. This phase was first lyophilized and then extracted from the dried material by ultrasound as described in the previous paragraph, followed by identification and quantification by GC.

2.8. Triton X-100 analysis

The GC analyses of control and surfactant-treated soil were compared to determine differences with the objective of identifying the peaks corresponding to Triton X-100. The chromatograms derived from hydrocarbon analysis were examined. The quantity of each identified peak from the surfactant-supplemented microcosms was then estimated by comparing the signal from that respective analyte with the peak from the internal standard.

2.9. Soil DNA extraction, PCR, and pyrosequencing of the 16S rRNA gene

The total DNA of each microcosm was extracted from 1 g of soil sample after 1, 14, and 63 days of incubation by means of the E.Z.N.A. Soil DNA Kit (Omega Bio-Tek, Inc., USA) following the manufacturer's instructions.

The PCR amplification was performed with the 16S rRNA universal bacterial primers, 341Fbac (5′-CCTACGGGAGGCAGCAG-3′) (Muyzer et al., 1993) and 909R (5′-CCCCGYCAATTCMTTTRAGT-3′) (Tamaki et al., 2011) in order to amplify a 568-bp fragment of the 16S-rRNA gene flanking the V3 and V4 regions, according to (Festa et al., 2016). After the PCR, the amplicon products from different samples were mixed in equal concentrations and purified by means of Agencourt Ampure beads (Agencourt Bioscience Corporation, USA). The samples were sequenced in a Roche 454 FLX titanium instrument and reagents according to the manufacturer's guidelines. This sequencing was carried out at the Molecular Research laboratory (MR DNA; Shallowater, TX) based upon established and validated protocols (http://www.mrdnalab.com/). Sequence data are available at the NCBI Sequence Read Archive (SRA) under the accession number PRJNA427682.

The sequence data derived from the high-throughput sequencing were analyzed employing a pipeline developed at Molecular Research LP (www.mrdnalab.com). Sequences were first depleted of bar codes and primers, then short sequences (<200 bp), those with ambiguous base calls, and those with homopolymer runs exceeding 6 bp were all deleted. The sequences were denoised and chimeras removed by means of custom software (Dowd et al., 2008b) and the Black Box Chimera Check software B2C2 (available at http://www.researchandtesting.com/B2C2.html). The rest were checked for high quality based on criteria utilized by the software RDP version 9 (Cole et al., 2009). Sequence data were clustered into operational taxonomic units (OTUs) with 3% divergence by means of the software uClust version v1.2.22. Those OTUs were then taxonomically classified by the BLASTn.NET algorithm (Dowd et al., 2005) against a database of high-quality bacterial 16S rRNA sequences derived from GreenGenes (10–2011 version) (Edgar, 2010). The outputs were compiled and validated through the use of taxonomic-distance methods (Dowd et al., 2008a, 2008b).

The resulting taxonomy was defined according to the following percentages: >97%, species; between 97% and 95%, unclassified genus; between 95% and 90%, unclassified family; between 90% and 85%, unclassified order; between 85% and 80%, unclassified class; between 80% and 77%, unclassified phylum; <77%, unclassified.

For the statistical analysis of the data, the Hill numbers—species richness (^0D), the exponential of the Shannon diversity index (^1D), and the reciprocal of the Simpson index (^2D) (Hill, 1973)—were used as estimates of diversity (Festa et al., 2016). The rarefaction curves were calculated by means of the EstimateS Version 9.1.0 software (http://viceroy.eeb.uconn.edu/EstimateS). Since these measurements were influenced by the sequencing depth, normalization was performed through resampling and diversity, with the estimation computed from 1059 sequences (corresponding to the number of reads in the shallowest-sampled

community) that were randomly drawn from each sample. A correspondence analysis (CA; NTSYSpc, version 2.11W) was performed on the pyrosequencing data based on the frequency values of each order. Bacterial-community profiles were also investigated though the construction of a heat map at the genus level by means of the R packages (R version 3.1.2). The clustering was based on the Bray–Curtis dissimilarity index, as calculated from the OTUs at a distance of 3%.

2.10. Real-time PCR

The gene-copy numbers of the eubacterial 16S-rRNA gene and the PAHs ring-hydroxylating α subunit-dioxygenase (PAH-RHDα) fragments were quantified by quantitative real-time PCR (qPCR) in a qTOWER 2.2™ Analytik Jena real-time PCR thermal cycler. The total DNA extracted from each microcosm at days 1, 14, and 63 was analyzed.

Bacterial 16S-rRNA gene was amplified using primers 1055f (5′-ATGGCTGTCGTCAGCT-3′) and 1392r (5′-AACGCGAAGAACCTTAC-3′) in order to amplify a 337-bp fragment (Harms et al., 2003). A PAH-RHDα subunit fragment for Gram-negative (GN) bacteria of 305 bp was amplified with the primers PAH-RHDαGNf (5′-GAGATGCATACCAC GTKGGTTGGA-3′) and PAH-RHDαGNr (5′-AGCTGTTGTTC GGGA AGAYWGTGCMGTT-3′) after Cébron et al. (2008). The PCR reactions were performed in 10-μl volumes containing 2× SYBR Green PCR Master Mix™ (Promega), 0.4 μM of each primer, 0.3 g l^{-1} of bovine-serum albumin, and 2 μl of the template DNA or distilled water for the negative control. The amplifications were carried out with the following temperature profiles: an initial heating to 95 °C (5 min), followed by 40 cycles of 3 steps for amplifying the 16S rRNA gene fragment and 50 cycles for the PAH-RHDαGN fragment. These steps were: 30 s of denaturation at 95 °C, 30 s at the primer's specific annealing temperature (53 °C and 57 °C for 16S rRNA gene and PAH-RHDα/GN amplification, respectively) and 30 s of elongation at 72 °C. The final step was for 7 min at 72 °C. At the end of the real-time PCR, a melting-curve analysis was performed by a final cycle that involved the measurement of the SYBR-Green–signal intensities for an initial step of 1 min at 95 °C, 30 s at the annealing temperature and 30 s at 95 °C. The quantifications were performed in triplicate qPCR runs.

Two plasmid standards with the corresponding target genes were cloned and purified and the sequences validated by a sequencing service (Macrogen, Korea). Dilutions of the corresponding standards were run together in triplicate with the samples. The Ct values of each standard dilution (*i.e.*, the number of cycles where the fluorescence data cross the threshold) were determined and plotted against the logarithm of the respective copy number per microliter in order to obtain the calibration curves. The Ct values of the environmental samples were determined and the target-gene copy number deduced from the standard curves.

The purity of the amplified PCR products was checked by: i) the observation of a single melting point during melting-curve analysis following the qPCR assays, and ii) the presence of a unique band of the expected size on 1% (w/v) molecular-grade agarose as visualized with a UV transilluminator (National Labnet Company, TM-26™) after staining the gel with 0.5 μg ml^{-1} ethidium bromide.

All results were processed by means of the MxPro-Mx3000P v4.10 qPCR software.

2.11. Statistical analysis

Statistical evaluations of the data from surface tension, PAH concentration, population size of heterotrophic bacteria and quantification of the 16S-rRNA gene and PAH-RHDα fragments were performed by a parametric one-way ANOVA followed by Tukey's *post-hoc* honestly-significant-difference test, by means of the XLStat-Pro statistical package v7.5.2.

3. Results

3.1. Determination of the CMC of Triton X-100 in PAH-contaminated soil suspensions

The CMC value calculated for IPK soil suspensions was 1056 mg l^{-1} (corresponding to 26 mg of Triton X-100 per g of dry soil), a concentration corresponding to a minimal surface tension of 32 mN m^{-1} (Fig. S1). According to this result, the microcosms T-A, T-B, and T-CMC were supplemented with 11, 14, and 26 mg g^{-1} of dry soil, respectively.

3.2. SEBR studies

3.2.1. Surface tension

Fig. 1 depicts the surface tension of soil suspensions obtained from the C, T-A, T-B, and T-CMC microcosms throughout the duration of the experiment. The addition of Triton X-100 produced a significant decrease ($P < 0.05$) in the surface tension of the T-A, T-B, and T-CMC microcosms relative to the C microcosm from the beginning of the incubation time and remained significantly lower until the end of the treatment. Although this decrease in the surface tension showed correlation with surfactant concentration, in the sub-CMC microcosms (T-A and T-B) the surface tension remained constant throughout the whole experiment. In contrast, the still lower values of surface tension in the T-CMC microcosm increased significantly ($P < 0.05$) after 63 days of treatment.

3.2.2. PAH biodegradation and desorption

Fig. 2 delineates the total (entire bars) and sorbed (filled bars) PAHs concentrations during the treatment in the C, T-A, T-B, and T-CMC microcosms. An initial notable decrease in PAHs concentration was observed at 7 days of treatment in all the microcosms, principally at the expense of the bioavailable fraction. Moreover, at this time the microcosms with sub-CMC doses (T-A and T-B) evidenced sorbed-PAHs concentrations significantly lower ($P < 0.05$) than those of the C group; thereafter, no further difference was found between the sorbed-PAHs fractions of the four microcosms at the subsequent treatment times.

In the C microcosms, the consumption of the PAHs-bioavailable fraction at day 7 was followed by a decrease in the sorbed fraction along with the reappearance of a bioavailable fraction (day 14), indicating that the abiotic-release rate was greater than the kinetics of biodegradation. When a sorbent contains PAHs and the degrading bacteria act as a withdrawal sink, that bacterial consumption drives the dissolution of the slowly desorbing fraction of PAHs from the sorbed pool (Johnsen et al., 2005).

After 42 days of treatment, the microcosms with sub-CMC surfactant doses exhibited a stimulation of PAHs degradation, having reached total-PAHs concentrations significantly lower ($P < 0.05$) than those of either the C or the T-CMC microcosms, with this decrease being attributable to a degradation of the bioavailable fraction. Fig. 3 exhibits the bioavailable and sorbed fractions of the individual PAHs that have been identified in the microcosms on day 42. The three surfactant concentrations resulted in more degradation of many PAHs than occurred in C. Whereas, in the T-CMC microcosm, the degradation of only the HMW PAHs occurred; at the sub-CMC doses, both HMW and LMW PAHs concentrations were reduced.

After 84 days of treatment the total PAHs concentration of the T-A and T-B microcosms consisted in only the sorbed-PAHs fraction, suggesting that in these microcosms the release of hydrocarbon from the sorbed fraction was rate-limiting for PAHs-degradation.

3.2.3. Triton-X-100 analysis

By comparing the chromatograms obtained from the control soil with those from the surfactant-supplemented soils, 10 peaks pertaining to Triton X-100 were identified (Fig. S2), that number resulting from the polydisperse nature of the ethylene-oxide units of the surfactant

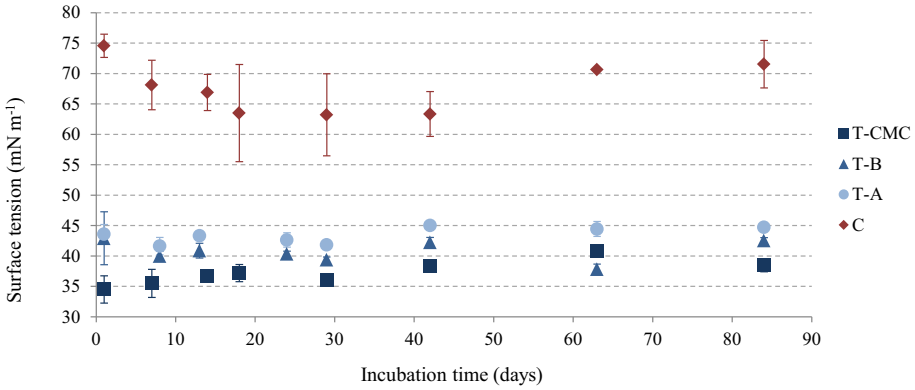

Fig. 1. Surface tension of soil suspensions of the four microcosms during the incubation period. The results are the means of triplicate independent microcosms with the bars representing the standard deviations.

(Franska et al., 2003). To determine the extent of Triton-X-100 degradation, the areas under these 10 peaks were compared in the chromatograms obtained from T-B and T-CMC after 1 and 84 days of treatment (Table 1).

The results demonstrated that the peaks with a longer retention time—thus constituting species of higher molecular weight (Franska et al., 2003)—were more extensively degraded (>90%) in the T-CMC microcosms. In that microcosm, the apparent lower degradation of the peaks with shorter retention times could have resulted from a reduction in the overall molecular weight of Triton X-100 via the sequential cleavage of the ethylene-oxide units (Chen et al., 2005) to produce a concomitant enrichment in the low molecular weight peaks.

In the T-B microcosm, the lower percent degradation of the peaks of higher retention time along with the disappearance of the peaks of low molecular weight would suggest a lower degree of Triton X-100 degradation.

3.2.4. Enumeration of populations of bacteria

From the beginning of the incubation time and during the first 21 days of treatment, no significant differences were found in the number of culturable heterotrophic bacteria among the four microcosms (except for T-A on the first day with a significantly lower count; Fig. 4, dashed lines); thereafter, and up to 63 days of incubation, the microcosm T-CMC manifested counts of heterotrophic bacteria significantly higher ($P < 0.05$) than the C microcosms. In contrast, the sub-CMC

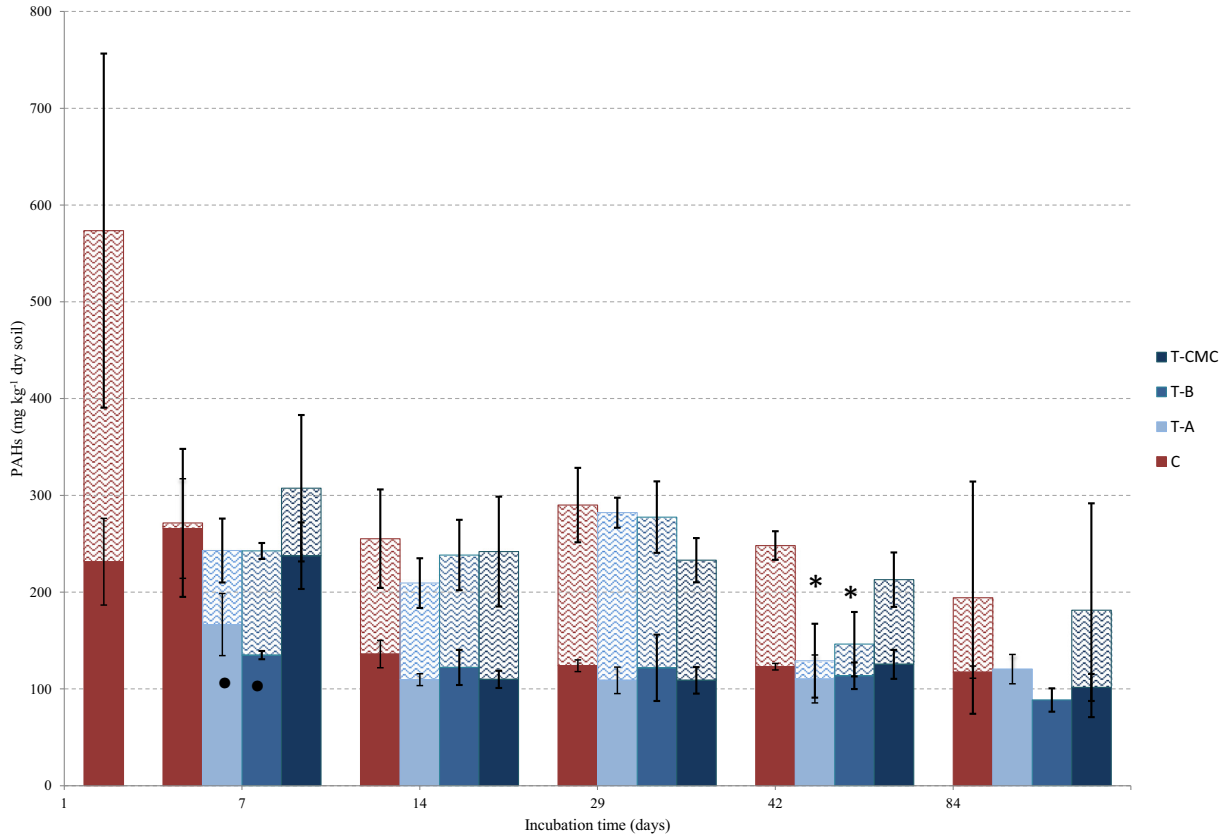

Fig. 2. Concentration of PAHs in the four microcosms during the incubation time. The entire bars correspond to the total PAHs concentration; the filled bar (■), the sorbed fraction; and the zig-zag striped bar (▨), the bioavailable fraction. The results are the means of triplicate independent microcosms with the brackets representing the standard deviations. The asterisk and circles indicate a significant difference between the control and the sorbed- or total-PAHs concentration, respectively.

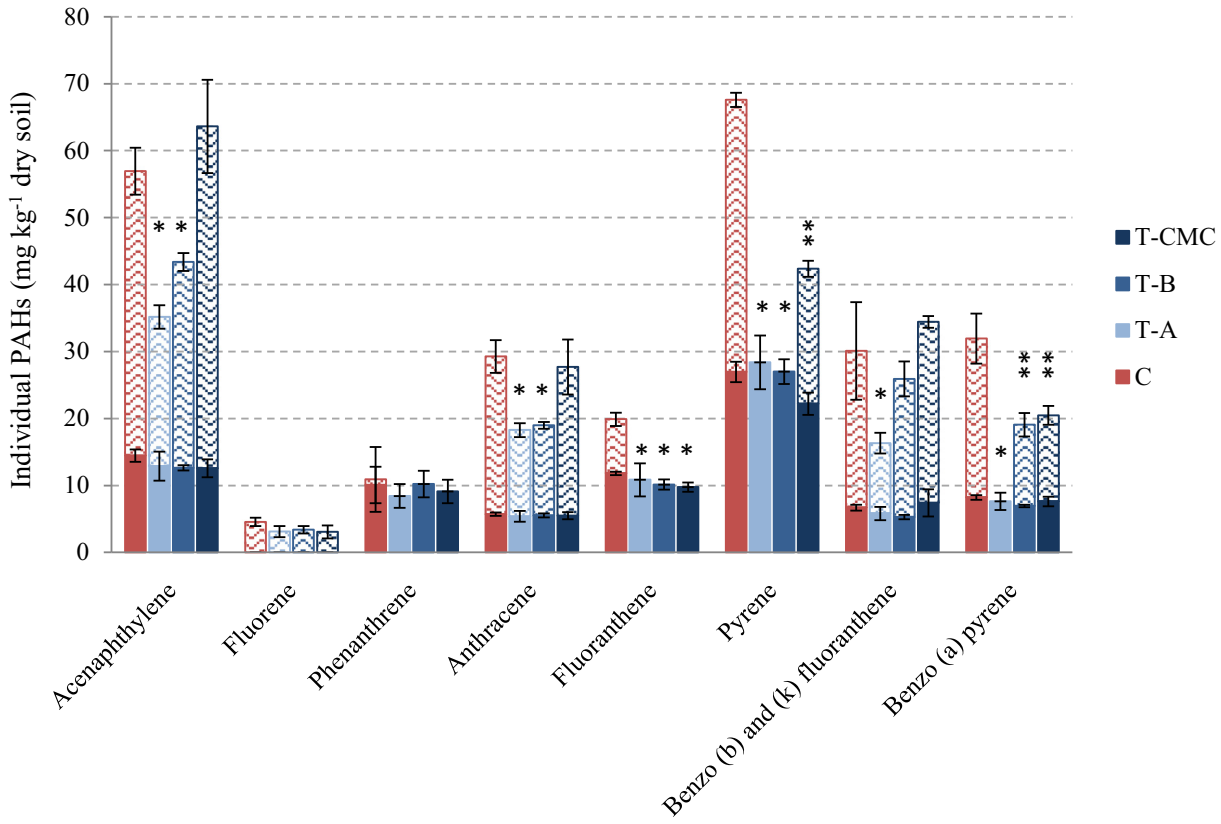

Fig. 3. Bioavailable (zig-zag striped bar, ▨) and sorbed (filled bar, ■) fractions of individual PAHs assayed on day 42. Each entire bar corresponds to the total PAHs concentration. The results are the means of triplicate independent microcosms with the brackets representing the standard deviations. The asterisks indicate a significant difference ($P < 0.05$) between the control and the surfactant treatments with respect to the total PAHs concentration.

microcosms contained significantly higher numbers ($P < 0.05$) than the C group only from day 42 until the end of the incubation. The quantification of the 16S-rRNA gene by qPCR (Fig. 4, solid lines) indicated no significant differences between the results with the control and the Triton X-100 microcosms during the initial stage, as was previously observed by bacterial cultivation. In addition, the copy numbers of 16S-rRNA gene in the surfactant microcosms registered at day 63 were significantly higher ($P < 0.05$) than those of the control.

With respect to the potential PAH-degrading capacity measured through the quantification of PAH-RHDα gene, no difference was found between the surfactant treatments and the control at the initial time (Fig. 5). Only after 42 days of incubation, did the T-A, T-B, and T-CMC microcosms contain a significantly higher ($P < 0.05$) ratio of PAH-RHDα/16S rRNA than the control.

3.2.5. Bacterial diversity, structure, and composition of the studied microcosms

The taxonomic composition and diversity of the bacterial microbiomes present in the soil microcosms on days 1, 14, and 63 of the experiment were profiled by the pyrosequencing of PCR-amplified bacterial 16S rRNA gene fragments. The number of sequences obtained ranged from 1059 to 8995 (Table S1) and were clustered into 1440 OTUs at a 97%-similarity threshold. The Good's-index coverage of all samples ranged from 0.84 to 0.99 (Table S1), and rarefaction analysis of the data (Fig. S3) indicated that the coverage achieved was enough to cover most of the diversity.

To assess the complexity of the soil bacterial communities, the Hill numbers were obtained (Fig. 6). Independently of the concentration, the addition of surfactant caused an immediate increase in the species

Table 1
Relative concentration of the ten peaks identified as Triton X-100, in the microcosms T-B and T-CMC, at days 1 and 84 of the incubation.

Triton-X-100 peaks (relative mg kg^{-1} dry soil)						
Retention time (min)	T-B			T-CMC		
	Day 1	Day 84	Elimination (%)[a]	Day 1	Day 84	Elimination (%)[a]
22.67	40.2 ± 0.7		100	27.7 ± 11.1	18.9 ± 3.3	31.8
26.95	5.5 ± 0.5		100	15.2 ± 2.6	2.6 ± 3.7	82.8
32.75	26.0 ± 1.5		100	28.3 ± 6.2	10.2 ± 1.5	64
35.34	16.1 ± 5.1		100	78.6 ± 17.7	7.3 ± 8.3	90.7
40.10	150.6 ± 40.9		100	786.3 ± 153.1	62.5 ± 11.0	92
42.20	251.9 ± 78.2		100	1278.9 ± 275.3	96.2 ± 4.8	92.5
44.62	319.6 ± 81.4	79.7 ± 35.5	75.10	1660.4 ± 357.2	136.1 ± 7.3	91.8
48.70	394.2 ± 117.0	123.4 ± 51.2	68.70	2021.5 ± 363.9	128.7 ± 15.0	93.6
56.01	367.7 ± 112.9	99.0 ± 26.8	73.10	1803.5 ± 268.6	63.6 ± 74.8	96.5
62.60	266.0 ± 93.3	109.2 ± 16.1	58.90	1348.3 ± 134.5	69.0 ± 4.4	94.9

Relative concentration values represent the arithmetic mean ± standard deviation of 3 replicates.
[a] Calculated at day 84 relative to day 1.

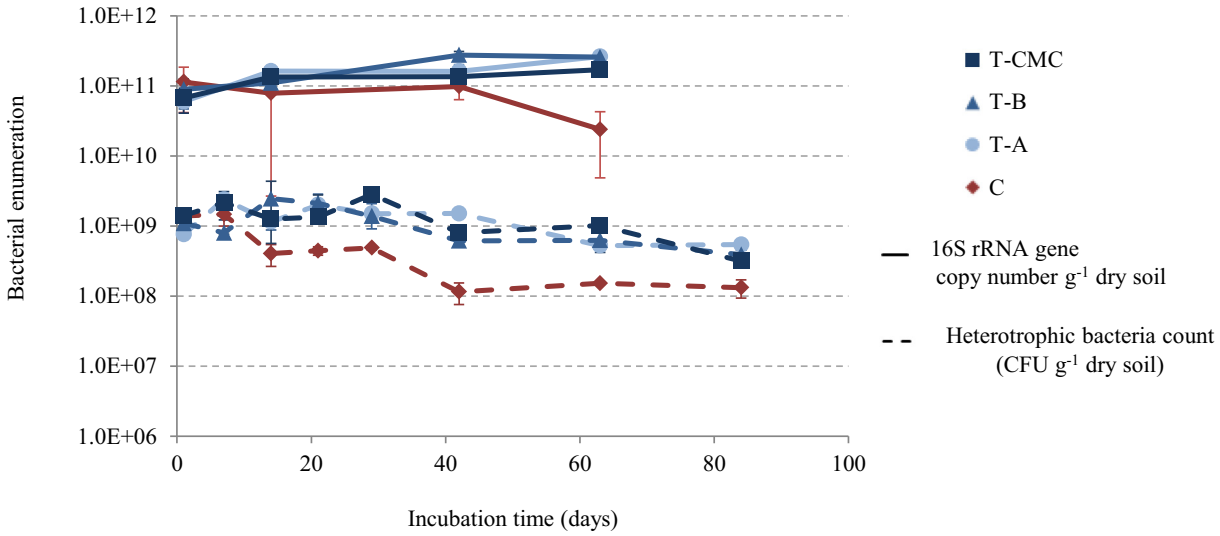

Fig. 4. Dynamics of the 16S-rRNA-gene copy numbers (solid lines) and the culturable heterotrophic bacteria (dashed lines) throughout the incubation period. The results are the means of triplicate independent microcosms with the brackets representing the standard deviations.

richness (^{0}D) and diversity (^{1}D and ^{2}D) of the soil bacterial community. This effect could be caused partially by an improvement in DNA recovery as a result of the surfactant influence on bacterial adhesion to hydrophobic soil surfaces (Fortin et al., 2004).

After 14 days of treatment, although the three surfactant-supplemented microcosms maintained the same species-richness levels along with a decrease in the diversity indices, indicating that some species became dominant; the C microcosm manifested a major increase in diversity and richness estimators. At 63 days of treatment, the C and T-CMC microcosms evidenced a decrease in the diversity indices along with a drop in the species richness, being quite drastic in the C microcosm.

The pyrosequencing results demonstrated that all the OTUs belonging to the four microcosms were classified in the domain Bacteria (15 phyla; Table S2). On average for the complete data set, the major microbial phyla were Proteobacteria (40.9%–88.5%), Actinobacteria (1.0%–31.2%), Firmicutes (0.6%–10.5%), Bacteroidetes (0.7%–6.4%), Chloroflexi (0.4%–12.0%), Acidobacteria (0%–5.9%), and Gemmatimonadetes (0%–5.0%).

To visualize the differences in community structure among the different microcosms at the level of order, a correspondence-analysis ordination plot of the unconstrained data was constructed (Fig. 7). The CA revealed pronounced differences in the soil bacterial community profiles within the C microcosm between days 1 and 63 and on day 14 of the incubation, indicating that the microcosm preparation (homogenization, sieving, and incubation) caused a marked but only temporary effect on the community profiles. The profile of the C.1 and C.63 samples are located on the right of zero on the *abscissa* (CA1) and are characterized by a predominance of the orders Bacillales and Pseudomonadales (Fig. 7).

The profiles from the C microcosm after 14 days of incubation along with the surfactant-amended microcosms at 1 and 14 days are situated near each other, on the left of zero on the *abscissa* and within the positive quadrant of the *ordinate* (CA2) of Fig. 7; indicating a greater contribution of the orders Acidimicrobiales, Actinomycetales, Cytophagales, Sphaerobacterales, Rhizobiales, Caulobacterales, Rhodospirillales, and Verrucomicrobiales.

After 63 days of incubation, the surfactant-containing microcosms exhibited a bacterial community profile notably different from that of the C microcosm; moreover, the profiles of the microcosms with sub-CMC surfactant doses (T-A and T-B) were separated from the T-CMC microcosm with respect to CA2 values. Whereas the T-A.63 and T-B.63 microcosms contained a high frequency of sequences belonging to the orders Acidobacteriales, Sphingomonadales, and Gemmatimonadales; the T-CMC.63 microcosm was characterized by a predominance of the order Xanthomonadales.

Fig. 8 depicts the hierarchically clustered heat-map analysis based on the bacterial-community profiles at the genus level, as obtained from the sequence frequencies of the 31 most abundant genera accounting for >70% of all the sequences.

The hierarchical heat-map analysis (Fig. 8) clearly identified two groups. The bacterial profile of all the microcosms at the initial time (day 1) formed a cluster (C1) distant from the surfactant-supplemented microcosms after 14 and 63 days of incubation and from the C microcosm after 14 days. The soil bacterial profile of the C microcosm after 63 days was clearly different from that of all other conditions.

The cluster formed by the samples at the initial time shared a highly similar community structure characterized by a prevalence of the *Brevundimonas*, *Nocardioides*, and *Acinetobacter* genera. Within this cluster, the profile of the C microcosm was distinguished by the dominance of the genera *Acinetobacter* and *Bacillus*.

The other cluster (C2) was composed of two subclusters, one formed by samples from all four microcosms at 14 days of incubation, which shared a highly similar community structure characterized by

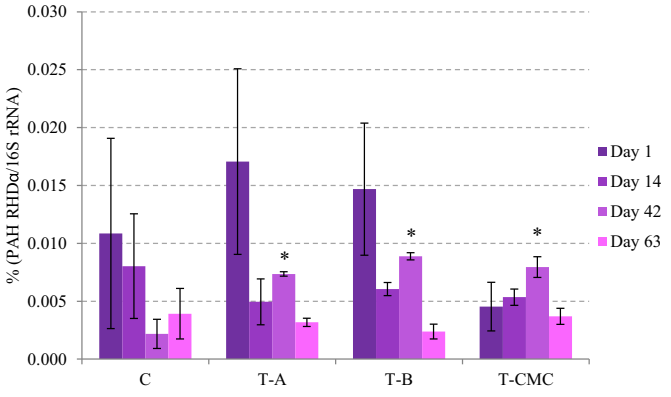

Fig. 5. The ratio of PAH-RHDα–gene-copy numbers to the 16S-rRNA–gene copy numbers for each microcosm. The figure represents the mean data along with the standard deviation in brackets from three independent DNA extractions. The asterisk signifies significant differences between the control and the surfactant treatments.

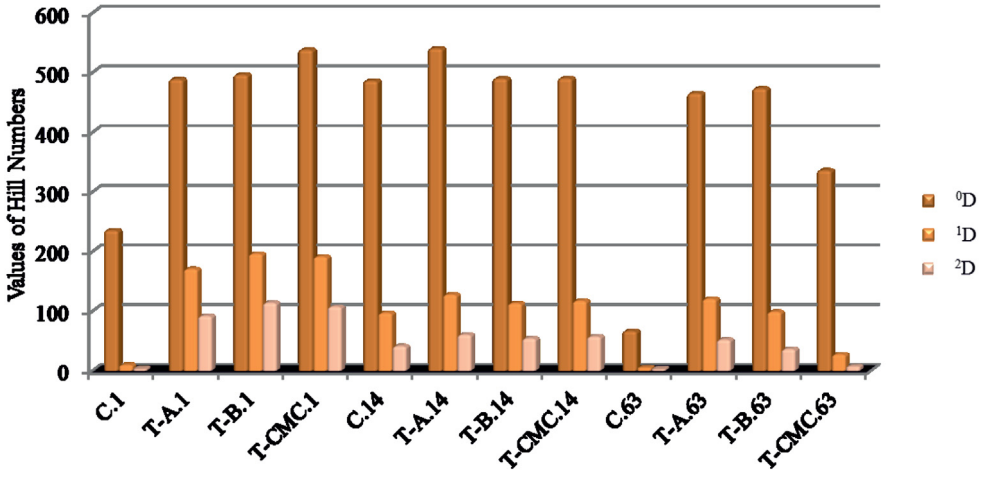

Fig. 6. Hill numbers for the different communities obtained by analysis of pyrosequencing through the use of the EstimateS program.

a prevalence of *Brevundimonas, Nocardioides*, *Sphingomonas*, *Xanthomonas*, and *Chloroflexus* among others (Fig. 8 and Table S4) plus a second containing the surfactant-supplemented microcosms after 63 days of incubation. Into this latter subcluster one branch was formed by the microcosms T-A and T-B, characterized by the prevalence of *Sphingomonas, Novosphingobium*, and *Brevundimonas*; whereas the other branch, formed by the microcosm T-CMC, was characterized by a marked prevalence of *Stenotrophomonas*.

4. Discussion

The effects of the nonionic surfactant Triton X-100 on PAHs degradation and desorption and on the soil bacterial community were evaluated at doses corresponding to the CMC and below the CMC in microcosms of an industrial soil chronically contaminated with PAHs. Optimization of the surfactant dose would improve the efficiency of the SEBR, thus minimizing the cost of treatment.

The dosage profile of the surfactant added produced a decrease in the surface tension of the soil suspension in relationship to the surfactant concentration (Fig. 1), confirming that the doses of the T-A and T-B microcosms were sub-CMC. Nevertheless, those microcosms, in which the micellar solubilization of PAHs would presumably be negligible, were the only ones that contained sorbed-PAHs concentrations significantly lower than that of the C microcosm at the beginning of the incubation (Fig. 2). That at sub-CMC doses the rate of PAHs desorption from a geosorbent could increase through a direct modification of the contaminant matrix is one possible explanation (Adrion et al., 2016). Moreover, Yeom et al. (1996) found that surfactants enhanced PAHs release from a soil they tested mainly by increasing the diffusivity of the matrix, with an increase in solubility through a partitioning of PAHs into the micellar pseudophase playing a secondary role. Our results would confirm this hypothesis since in the T-CMC microcosm, where most surfactant molecules would be aggregated into micelles, the sorbed PAHs concentration was no different from that of the control (Fig. 2).

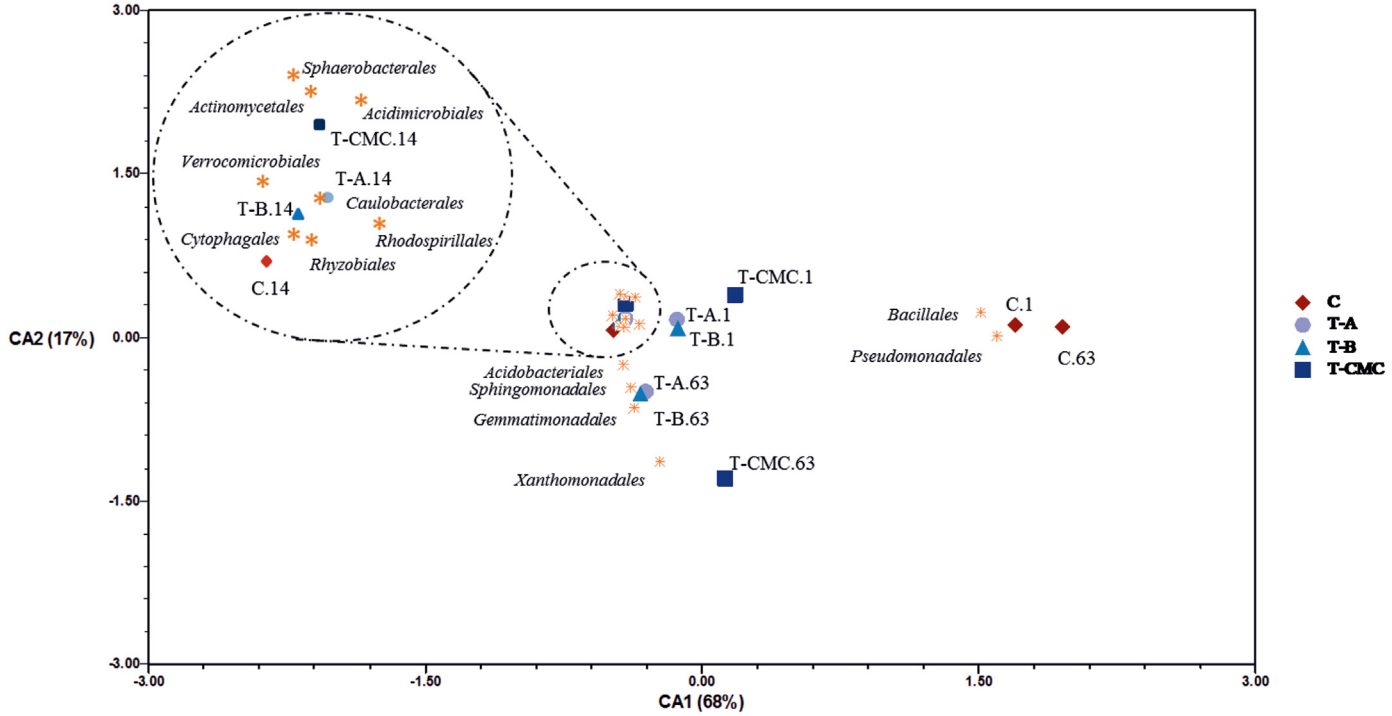

Fig. 7. Correspondence analysis based on the frequency of orders within the bacterial diversity in the four microcosms.

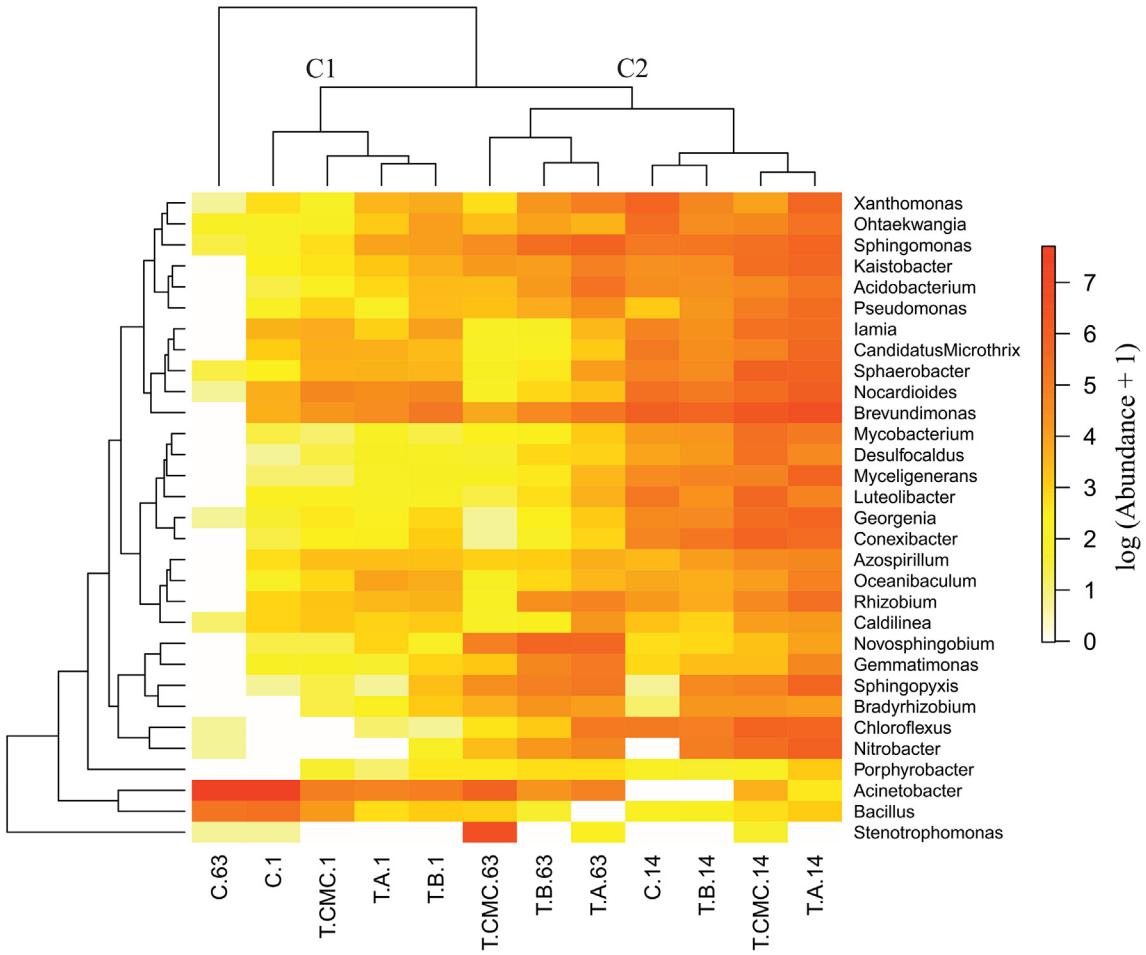

Fig. 8. Heat-map plot depicting the frequency of each bacterial genus (variables clustering on the *ordinate* within each sample on the *abscissa*). The values in the heat map represent the log-transformed abundance (Log X + 1) of each bacterial genus, indicated by the color intensity as displayed on the right side of the figure. Bacterial distribution among the four microcosms is denoted by a double hierarchical dendrogram. The bacterial phylogenetic cluster and the relationship among the samples were determined by the Bray-Curtis distance and the complete-clustering method.

In addition to mobilizing matrix-sorbed hydrophobic compounds, surfactants can also impact the PAHs-degrading activity of the endogenous microbial community in a contaminated environment (Makkar and Rockne, 2003). Although few attempts have been undertaken to evaluate this changes, evidence for a biologic contribution to the improvement of PAHs degradation has been reported (Singleton et al., 2016). Our results—obtained through high-throughput sequencing of 16S rRNA amplicons of soil DNA (Fig. 8)—demonstrated that the bacterial-community structure and dynamics were notably different between the C, T-CMC, and sub-CMC microcosms. This observation could be correlated with the difference in the elimination of bioavailable-PAHs fraction observed after 42 days of incubation (Fig. 2). In addition, those differences could have produced the varied degradation profile observed on day 42. Whereas, in the sub-CMC microcosms, the levels of LMW and HMW PAHs remaining were lower than those in the controls, the differences in the residual-PAHs concentrations between the T-CMC microcosms and the control were only with respect to the high-molecular-weight species (Fig. 3). In previous SEBR studies (Adrion et al., 2016; Zhu and Aitken, 2010), differences in PAHs degradation have been attributed to the impact of the surfactants used on the microbial community.

In the C microcosm, the preparation and incubation conditions produced an increase in species richness and diversity of the bacterial community followed by a drastic reduction in those parameters (Fig. 6). Thomson et al. (2010), using molecular fingerprinting (T-RFLP), found that the method of sieving and homogenization significantly altered the soil bacterial community structure. In the chronically contaminated soil studied here, the inaccessible PAHs entrapped within the soil aggregates could have been exposed to the soil microbiome by the sieving procedure. In concordance with that possibility, the analytical results indicated that immediately after microcosm preparation the PAHs-bioavailable fraction represented the greater proportion (60%; Fig. 2), though that fraction became subsequently degraded by the extant microbial community strongly selected by the preexisting contamination (Figs. 7 and 8). The species of the *Acinetobacter* and *Bacillus* genera, which taxa dominated the community of C microcosms at the beginning of the incubation time, had previously been found to possess hydrocarbon-degrading capabilities (Astashkina et al., 2015; Brzeszcz et al., 2016; Golby et al., 2012; Wu et al., 2017).

The addition of surfactant, at any of the concentrations used here, effected notable changes in the dynamics of the bacterial soil community compared to the status of the C microcosm (Figs. 6 and 7); as a result, after 63 days of incubation, the bacterial communities of the surfactant-containing microcosms were substantially different in diversity (Fig. 6) and composition (Fig. 8) from those of the C microcosm. Indeed, between 14 and 63 days of incubation, the profile of the soil bacterial community of microcosm T-CMC diverged from those of the sub-CMC microcosms (Figs. 7 and 8), in a manner consistent with the degree of PAHs degradation (Fig. 2).

After 63 days of treatment, the bacterial-community profiles of the T-A and T-B microcosms contained a predominance of the orders Sphingomonadales, Acidobacteriales, and Gemmatimonadales (Fig. 7). Consistent with the stimulation of PAHs degradation in the sub-CMC microcosms occurring after 42 days of incubation (Fig. 2), the relative abundance of PAH-RHDα genes (Fig. 5) indicated an increase in the PAHs-biodegradation potential of the community. In addition, the pyrosequencing results demonstrated an increase in the relative abundance of bacterial groups with known PAHs-degrading capabilities and/or those that had been previously detected as key components in the PAHs-degrading microbial community. The order Sphingomonadales, mainly represented by the genera *Sphingomonas* and *Novosphingobium* (Fig. 8 and Table S4), has been singled out as a fundamental clade involved in the biodegradation of PAHs (Bastida et al., 2016; Festa et al., 2016). Thus, Jiang et al. (2015), using DNA-stable isotope probing, demonstrated that the Acidobacteria-related bacteria were linked with PAHs degradation. Although the recently described phylum Gemmatimonadetes has few cultivable representatives, certain studies have shown that this phylum has been present in PAHs-polluted soils (Muangchinda et al., 2015; Tejeda-Agredano et al., 2013).

On day 63 of the incubation, the bacterial community of the T-CMC microcosm—characterized by a lower richness and diversity index compared to those of the T-A and T-B microcosms (Fig. 6), with a marked predominance of the order Xantomonadales (Fig. 5)—was mainly represented by the *Stenotrophomonas* genus. Other studies had described the inhibition of microbial PAHs-degrading activity by nonionic surfactants at concentrations above the CMC (Lladó et al., 2015; Singleton et al., 2016), which effect is probably caused by a physicochemical interaction between the surfactant micelle and the bacterial cell-walls, effecting a disruption of the membrane lamellar structure (Liu et al., 2016). Nevertheless, strains of the *Stenotrophomonas* genus have been reported as PAHs- (Koshlaf and S Ball, 2017; Lim et al., 2016) and Triton X-100- (Chen et al., 2004) degrading bacteria. The evidence of a higher Triton X-100 degradation in the T-CMC microcosm (Table 1), which result agrees with the increase in the surface tension observed in that microcosm after 63 days of treatment (Fig. 1), could be an indication of Triton X-100 biodegradation by a highly selected bacterial community—it therefore having a negative impact on PAHs biodegradation.

5. Conclusion

Our study demonstrated that the addition of Triton X-100 to a chronically contaminated soil enhanced the PAHs biodegradation only at sub-CMC concentrations. A similar result had been found by Singleton et al. (2016), in a soil bioreactor with another nonionic surfactant (Brij 30). The chemical determination of the sorbed and bioavailable PAHs fractions in combination with the use of pyrosequencing—a powerful tool for analyzing complex microbial communities—enabled us to obtain strong evidence for the involvement of both physicochemical and biological influences determining the different behaviors of the experimental microcosms that we recorded. The details elucidated in this work will no doubt contribute significantly to the optimization of SEBR strategies.

Acknowledgements

This work was supported by the Agencia Nacional de Promoción Científica y Tecnológica (PICT 2013-0103) and PIO CONICET-Fundación YPF (N° 13320130100005CO). M. Cecotti is doctoral fellow of CONICET. V. Mora, M. Viera, and B. Coppotelli are research members of CONICET. I. S. Morelli is research members of the CIC-PBA. Dr. Donald F. Haggerty, a retired academic career investigator and native English speaker, edited the manuscript.

Appendix A. Supplementary data

Supplementary data to this article can be found online at https://doi.org/10.1016/j.scitotenv.2018.03.303.

References

Adrion, A.C., Nakamura, J., Shea, D., Aitken, M.D., 2016. Screening nonionic surfactants for enhanced biodegradation of polycyclic aromatic hydrocarbons remaining in soil after conventional biological treatment. Environ. Sci. Technol. 50:3838–3845. https://doi.org/10.1021/acs.est.5b05243.

Astashkina, A.P., Bakibayev, A.A., Plotnikov, E.V., Kolbysheva, Y.V., Mukashev, A.B., 2015. Study of the hydrocarbon-oxidizing activity of bacteria of the genera Pseudomonas and Rhodococcus. Procedia Chem. 15:90–96. https://doi.org/10.1016/j.proche.2015.10.014.

Bastida, F., Jehmlich, N., Lima, K., Morris, B.E.L., Richnow, H.H., Hernández, T., von Bergen, M., García, C., 2016. The ecological and physiological responses of the microbial community from a semiarid soil to hydrocarbon contamination and its bioremediation using compost amendment. J. Proteome 135:162–169. https://doi.org/10.1016/j.jprot.2015.07.023.

Bezza, F.A., Chirwa, E.M.N., 2017. The role of lipopeptide biosurfactant on microbial remediation of aged polycyclic aromatic hydrocarbons (PAHs)-contaminated soil. Chem. Eng. J. 309:563–576. https://doi.org/10.1016/j.cej.2016.10.055.

Brzeszcz, J., Steliga, T., Kapusta, P., Turkiewicz, A., Kaszycki, P., 2016. R-strategist versus K-strategist for the application in bioremediation of hydrocarbon-contaminated soils. Int. Biodeterior. Biodegrad. 106:41–52. https://doi.org/10.1016/j.ibiod.2015.10.001.

Bueno-Montes, M., Springael, D., Ortega-Calvo, J.J., 2011. Effect of a nonionic surfactant on biodegradation of slowly desorbing PAHs in contaminated soils. Environ. Sci. Technol. 45:3019–3026. https://doi.org/10.1021/es1035706.

Cébron, A., Norini, M.P., Beguiristain, T., Leyval, C., 2008. Real-time PCR quantification of PAH-ring hydroxylating dioxygenase (PAH-RHDα) genes from Gram positive and Gram negative bacteria in soil and sediment samples. J. Microbiol. Methods 73:148–159. https://doi.org/10.1016/j.mimet.2008.01.009.

Chen, H.J., Huang, S.L., Tseng, D.H., 2004. Aerobic biotransformation of octylphenol polyethoxylate surfactant in soil microcosms. Environ. Technol. 25:201–210. https://doi.org/10.1080/09593330409355453.

Chen, H.-J., Tseng, D.-H., Huang, S.-L., 2005. Biodegradation of octylphenol polyethoxylate surfactant Triton X-100 by selected microorganisms. Bioresour. Technol. 96:1483–1491. https://doi.org/10.1016/j.biortech.2004.11.013.

Cole, J.R., Wang, Q., Cardenas, E., Fish, J., Chai, B., Farris, R.J., Kulam-Syed-Mohideen, A.S., McGarrell, D.M., Marsh, T., Garrity, G.M., Tiedje, J.M., 2009. The ribosomal database project: improved alignments and new tools for rRNA analysis. Nucleic Acids Res. 37:D141–D145. https://doi.org/10.1093/nar/gkn879.

Colores, G.M., Macur, R.E., Ward, D.M., Inskeep, W.P., 2000. Molecular analysis of surfactant-driven microbial population shifts in hydrocarbon contaminated soils. Appl. Environ. Microbiol. 66:2959. https://doi.org/10.1128/AEM.66.7.2959-2964.2000.

de la Cueva, S.C., Hernández-Rodríguez, C., Soto-Cruz, N.O., Rojas Contreras, J.A., López Miranda, J., 2016. Changes in bacterial populations during bioremediation of soil contaminated with petroleum hydrocarbons. Water Air Soil Pollut. 227. https://doi.org/10.1007/s11270-016-2789-z.

Dowd, S.E., Zaragoza, J., Rodriguez, J.R., Oliver, M.J., Payton, P.R., 2005. Windows .NET network distributed basic local alignment search toolkit (W.ND-BLAST). BMC Bioinforma. 6. https://doi.org/10.1186/1471-2105-6-93.

Dowd, S.E., Callaway, T.R., Wolcott, R.D., Sun, Y., McKeehan, T., Hagevoort, R.G., Edrington, T.S., 2008a. Evaluation of the bacterial diversity in the feces of cattle using 16S rDNA bacterial tag-encoded FLX amplicon pyrosequencing (bTEFAP). BMC Microbiol. 8. https://doi.org/10.1186/1471-2180-8-125.

Dowd, S.E., Sun, Y., Wolcott, R.D., Domingo, A., Carroll1, J.A., 2008b. Bacterial tag—encoded FLX amplicon pyrosequencing (bTEFAP) for microbiome studies: bacterial diversity in the ileum of newly weaned salmonella-infected pigs. Foodborne Pathog. Dis. 5. https://doi.org/10.1089/fpd.2008.0107.

Edgar, R.C., 2010. Search and clustering orders of magnitude faster than BLAST. Bioinformatics 26:2460–2461. https://doi.org/10.1093/bioinformatics/btq461.

Festa, S., Coppotelli, B.M., Morelli, I.S., 2016. Comparative bioaugmentation with a consortium and a single strain in a phenanthrene-contaminated soil: impact on the bacterial community and biodegradation. Appl. Soil Ecol. 98:8–19. https://doi.org/10.1016/j.apsoil.2015.08.025.

Fortin, N., Beaumier, D., Lee, K., Greer, C.W., 2004. Soil washing improves the recovery of total community DNA from polluted and high organic content sediments. J. Microbiol. Methods 56:181–191. https://doi.org/10.1016/j.mimet.2003.10.006.

Franska, M., Franski, R., Szymanski, A., Lukaszewski, Z., 2003. A central fission pathway in alkylphenol ethoxylate biodegradation. Water Res. 37:1005–1014. https://doi.org/10.1016/S0043-1354(02)00444-X.

Ghosh, I., Mukherji, S., 2016. Diverse effect of surfactants on pyrene biodegradation by a Pseudomonas strain utilizing pyrene by cell surface hydrophobicity induction. Int. Biodeterior. Biodegrad. 108:67–75. https://doi.org/10.1016/j.ibiod.2015.12.010.

Golby, S., Ceri, H., Gieg, L.M., Chatterjee, I., Marques, L.L.R., Turner, R.J., 2012. Evaluation of microbial biofilm communities from an Alberta oil sands tailings pond. FEMS Microbiol. Ecol. 79:240–250. https://doi.org/10.1111/j.1574-6941.2011.01212.x.

Harms, G., Layton, A.C., Dionisi, H.M., Gregory, I.R., Garrett, V.M., Hawkins, S.A., Robinson, K.G., Sayler, G.S., 2003. Real-time PCR quantification of nitrifying bacteria in a municipal wastewater treatment plant. Environ. Sci. Technol. 37:343–351. https://doi.org/10.1021/es0257164.

Hill, M.O., 1973. Diversity and evenness: a unifying notation and its consequences. Ecology 54, 427–432.
Jiang, L., Song, M., Luo, C., Zhang, D., Zhang, G., 2015. Novel Phenanthrene-degrading Bacteria identified by DNA-stable isotope probing. PLoS One 10. https://doi.org/10.1371/journal.pone.0130846.
Johnsen, A.R., Wick, L.Y., Harms, H., 2005. Principles of microbial PAH-degradation in soil. Environ. Pollut. 133:71–84. https://doi.org/10.1016/j.envpol.2004.04.015.
Koshlaf, E., S Ball, A., 2017. Soil bioremediation approaches for petroleum hydrocarbon polluted environments. AIMS Microbiol. 3:25–49. https://doi.org/10.3934/microbiol.2017.1.25.
Lamichhane, S., Bal Krishna, K.C., Sarukkalige, R., 2017. Surfactant-enhanced remediation of polycyclic aromatic hydrocarbons: a review. J. Environ. Manag. 199:46–61. https://doi.org/10.1016/j.jenvman.2017.05.037.
Lim, M.W., Von Lau, E., Poh, P.E., 2016. A comprehensive guide of remediation technologies for oil contaminated soil — present works and future directions. Mar. Pollut. Bull. 109:14–45. https://doi.org/10.1016/j.marpolbul.2016.04.023.
Liu, S., Guo, C., Liang, X., Wu, F., Dang, Z., 2016. Nonionic surfactants induced changes in cell characteristics and phenanthrene degradation ability of Sphingomonas sp. GY2B. Ecotoxicol. Environ. Saf. 129:210–218. https://doi.org/10.1016/j.ecoenv.2016.03.035.
Lladó, S., Covino, S., Solanas, A.M., Viñas, M., Petruccioli, M., D'annibale, A., 2013. Comparative assessment of bioremediation approaches to highly recalcitrant PAH degradation in a real industrial polluted soil. J. Hazard. Mater. 248:407–414. https://doi.org/10.1016/j.jhazmat.2013.01.020.
Lladó, S., Covino, S., Solanas, A.M., Petruccioli, M., D'annibale, A., Viñas, M., 2015. Pyrosequencing reveals the effect of mobilizing agents and lignocellulosic substrate amendment on microbial community composition in a real industrial PAH-polluted soil. J. Hazard. Mater. 283:35–43. https://doi.org/10.1016/j.jhazmat.2014.08.065.
Luque-García, J.L., Luque De Castro, M.D., 2003. Ultrasound: a powerful tool for leaching. TrAC Trends Anal. Chem. 22:41–47. https://doi.org/10.1016/S0165-9936(03)00102-X.
Makkar, R.A.S.M., Rockne, K.J., 2003. Comparison of synthetic surfactants and biosurfactants in enhancing biodegradation of polycyclic aromatic hydrocarbons. Environ. Toxicol. Chem. 22:2280–2292. https://doi.org/10.1897/02-472.
Mao, X., Jiang, R., Xiao, W., Yu, J., 2015. Use of surfactants for the remediation of contaminated soils: a review. J. Hazard. Mater. 285:419–435. https://doi.org/10.1016/j.jhazmat.2014.12.009.
Medina, R., Rosso, J.A., Del Panno, M.T., 2017. Remediación de un suelo crónicamente contaminado con Hidrocarburos Policíclicos Aromáticos.
Mora, V.C., Madueño, L., Peluffo, M., Rosso, J.A., Del Panno, M.T., Morelli, I.S., 2014. Remediation of phenanthrene-contaminated soil by simultaneous persulfate chemical oxidation and biodegradation processes. Environ. Sci. Pollut. Res. 21:7548–7556. https://doi.org/10.1007/s11356-014-2687-0.
Morelli, I.S., Del Panno, M.T., De Antoni, G.L., Painceira, M.T., 2005. Laboratory study on the bioremediation of petrochemical sludge-contaminated soil. Int. Biodeterior. Biodegrad. 55:271–278. https://doi.org/10.1016/j.ibiod.2005.03.001.
Muangchinda, C., Chavanich, S., Viyakarn, V., Watanabe, K., Imura, S., Vangnai, A.S., Pinyakong, O., 2015. Abundance and diversity of functional genes involved in the degradation of aromatic hydrocarbons in Antarctic soils and sediments around Syowa Station. Environ. Sci. Pollut. Res. 22:4725–4735. https://doi.org/10.1007/s11356-014-3721-y.
Muyzer, G., De Waal, E.C., Uitierlinden, A.G., 1993. Profiling of complex microbial populations by denaturing gradient gel electrophoresis analysis of polymerase chain reaction-amplified genes coding for 16S rRNA. Appl. Environ. Microbiol. 59, 695–700.
Northcott, G.L., Jones, K.C., 2001. Partitioning, extractability, and formation of nonextractable PAH residues in soil. 2. Effects on compound dissolution behavior. Environ. Sci. Technol. 35:1111–1117. https://doi.org/10.1021/es000072q.
Ortega-Calvo, J.J., Tejeda-Agredano, M.C., Jimenez-Sanchez, C., Congiu, E., Sungthong, R., Niqui-Arroyo, J.L., Cantos, M., 2013. Is it possible to increase bioavailability but not environmental risk of PAHs in bioremediation? J. Hazard. Mater. 261:733–745. https://doi.org/10.1016/j.jhazmat.2013.03.042.
Reasoner, D.J., Geldreich, E.E., 1985. A new medium for the enumeration and subculture of bacteria from potable water. Appl. Environ. Microbiol. 49, 1–7.
Ren, X., Zeng, G., Tang, L., Wang, J., Wan, J., Liu, Y., Yu, J., Yi, H., Ye, S., Deng, R., 2017. Sorption, transport and biodegradation – An insight into bioavailability of persistent organic pollutants in soil. Sci. Total Environ.:1154–1163 https://doi.org/10.1016/j.scitotenv.2017.08.089.
Singleton, D.R., Adrion, A.C., Aitken, M.D., 2016. Surfactant-induced bacterial community changes correlated with increased polycyclic aromatic hydrocarbon degradation in contaminated soil. Appl. Microbiol. Biotechnol. 100:10165–10177. https://doi.org/10.1007/s00253-016-7867-z.
Sun, M., Luo, Y., Christie, P., Jia, Z., Li, Z., Teng, Y., 2012. Methyl-β-cyclodextrin enhanced biodegradation of polycyclic aromatic hydrocarbons and associated microbial activity in contaminated soil. J. Environ. Sci. 24:926–933. https://doi.org/10.1016/S1001-0742(11)60865-6.
Tamaki, H., Wright, C.L., Li, X., Lin, Q., Hwang, C., Wang, S., Thimmapuram, J., Kamagata, Y., Liu, W.-T., 2011. Analysis of 16S rRNA amplicon sequencing options on the Roche/454 next-generation titanium sequencing platform. PLoS One 6:1–6. https://doi.org/10.1371/journal.pone.0025263.
Tejeda-Agredano, M.C., Gallego, S., Vila, J., Grifoll, M., Ortega-Calvo, J.J., Cantos, M., 2013. Influence of the sunflower rhizosphere on the biodegradation of PAHs in soil. Soil Biol. Biochem. 57, 830–840.
Thomson, B.C., Ostle, N.J., McNamara, N.P., Whiteley, A.S., Griffiths, R.I., 2010. Effects of sieving, drying and rewetting upon soil bacterial community structure and respiration rates. J. Microbiol. Methods 83:69–73. https://doi.org/10.1016/j.mimet.2010.07.021.
Wang, L., Li, F., Zhan, Y., Zhu, L., 2016. Shifts in microbial community structure during in situ surfactant-enhanced bioremediation of polycyclic aromatic hydrocarbon-contaminated soil. Environ. Sci. Pollut. Res. https://doi.org/10.1007/s11356-016-6630-4.
Wu, M., Ye, X., Chen, K., Li, W., Yuan, J., Jiang, X., 2017. Bacterial community shift and hydrocarbon transformation during bioremediation of short-term petroleum-contaminated soil. Environ. Pollut. 223:657–664. https://doi.org/10.1016/j.envpol.2017.01.079.
Yeom, I.T., Ghosh, M.M., Cox, C.D., 1996. Kinetic aspects of surfactant solubilization of soil-bound polycyclic aromatic hydrocarbons. Environ. Sci. Technol. 30:1589–1595. https://doi.org/10.1021/es950567t.
Yu, S., Li, S., Tang, Y., Wu, X., 2011. Succession of bacterial community along with the removal of heavy crude oil pollutants by multiple biostimulation treatments in the Yellow River Delta, China. J. Environ. Sci. 23:1533–1543. https://doi.org/10.1016/S1001-0742(10)60585-2.
Zhu, H., Aitken, M.D., 2010. Surfactant-enhanced desorption and biodegradation of polycyclic aromatic hydrocarbons in contaminated soil. Environ. Sci. Technol. 44:7260–7265. https://doi.org/10.1021/es100112a.